10/506859 PCT/IL02/00664

PA 913283

THE UNITED STATES OF AMERICA

TO ALL TO WHOM THESE PRESENTS SHALL COME:

UNITED STATES DEPARTMENT OF COMMERCE

United States Patent and Trademark Office

October 22, 2002

THIS IS TO CERTIFY THAT ANNEXED HERETO IS A TRUE COPY FROM THE RECORDS OF THE UNITED STATES PATENT AND TRADEMARK OFFICE OF THOSE PAPERS OF THE BELOW IDENTIFIED PATENT APPLICATION THAT MET THE REQUIREMENTS TO BE GRANTED A FILING DATE UNDER 35 USC 111.

APPLICATION NUMBER: ***60/363,947***
FILING DATE: ***March 14, 2002***

PRIORITY DOCUMENT
SUBMITTED OR TRANSMITTED IN COMPLIANCE WITH RULE 17.1(a) OR (b)

By Authority of the
COMMISSIONER OF PATENTS AND TRADEMARKS

M. SIAS
Certifying Officer

03/14/02 PTO

Please type a plus sign (+) inside this box → +

PTO/ SB/16 (8-00)
Approved for use through 10/31/2002. OMB 0651-0032
U.S. Patent and Trademark Office: U.S. DEPARTMENT OF COMMERCE
Under the Paperwork Reduction Act of 1995, no persons are required to respond to a collection of information unless it displays a valid OMB control number.

01050 U.S. PTO 60/363947 03/14/02

PROVISIONAL APPLICATION FOR PATENT COVER SHEET

This is a request for filing a PROVISIONAL APPLICATION FOR PATENT under 37 CFR 1.53(c).

INVENTOR(S)

Given Name (first and middle (if any))	Family Name or Surname	Residence (City and either State or Foreign Country)
Varda	HERSKOWITS	Petach-Tikva, Israel
Antony J.	WEISS	Tel-Aviv, Israel
Menachem	TIPRIS	Raanana, Israel
Shmuel	LEVY	Kiryat-Tivon, Israel

☐ *Additional inventors are being named on the ____ separately numbered sheets attached hereto*

TITLE OF THE INVENTION (280 characters max)

BROADBAND OPTICAL EQUALIZER

Direct all correspondence to: **CORRESPONDENCE ADDRESS**

☐ Customer Number [ ] → *Place Customer Number Bar Code Label here*

OR *Type Customer Number here*

☒ Firm or Individual Name	Roy N. Envall, Jr.				
Address	c/o Anthony Castorina				
Address	2001 Jefferson Davis Highway, Suite 207				
City	Arlington	State	VA	ZIP	22202
Country	U.S.A.	Telephone	(703) 415-1581	Fax	(703) 415-4884

ENCLOSED APPLICATION PARTS *(check all that apply)*

☒ Specification *Number of Pages* 17
☐ Drawing(s) ~~Number of Sheets~~ included in spec.
☐ Application Data Sheet. See 37 CFR 1.76
☐ CD(s), Number
☐ Other (specify)

METHOD OF PAYMENT OF FILING FEES FOR THIS PROVISIONAL APPLICATION FOR PATENT *(check one)*

☒ Applicant claims small entity status. See 37 CFR 1.27.
☐ A check or money order is enclosed to cover the filing fees
☒ The Commissioner is hereby authorized to charge filing fees or credit any overpayment to Deposit Account Number: 03-3419
☐ Payment by credit card. Form PTO-2038 is attached.

FILING FEE AMOUNT ($): $80.00

The invention was made by an agency of the United States Government or under a contract with an agency of the United States Government.

☒ No.
☐ Yes, the name of the U.S. Government agency and the Government contract number are: _____

Respectfully submitted,

SIGNATURE Paul Fenster

Date 03/14/2002

TYPED or PRINTED NAME Paul Fenster

REGISTRATION NO. (if appropriate) 33,877

Docket Number: 306/02554

TELEPHONE (703) 415-1581

USE ONLY FOR FILING A PROVISIONAL APPLICATION FOR PATENT

This collection of information is required by 37 CFR 1.51. The information is used by the public to file (and by the PTO to process) a provisional application. Confidentiality is governed by 35 U.S.C. 122 and 37 CFR 1.14. This collection is estimated to take 8 hours to complete, including gathering, preparing, and submitting the complete provisional application to the PTO. Time will vary depending upon the individual case. Any comments on the amount of time you require to complete this form and/or suggestions for reducing this burden, should be sent to the Chief Information Officer, U.S. Patent and Trademark Office, U.S. Department of Commerce, Washington, D.C. 20231. DO NOT SEND FEES OR COMPLETED FORMS TO THIS ADDRESS. SEND TO: Box Provisional Application, Assistant Commissioner for Patents, Washington, D.C.

PTOS ALL/REV05

306/02555

BROADBAND OPTICAL EQUALIZER

Background

An optical pulse traveling along a communication link comprised of single mode fibers and various devices such as amplifiers, mux/demux, add/drop etc., is affected by static and dynamic dispersion resulting in pulse spreading, which may impair detection and increase the BER. In general, the dispersion induced spreading is wavelength dependent, or otherwise stated, the pulse spread is, among others, proportional to the signal bandwidth determined by the pulse-width. Polarization mode dispersion [PMD] constitutes one of the major sources of dynamic pulse spreading. Time dependent residual chromatic dispersion [RCD] and non-linear effects such as cross phase modulation constitute additional sources of dynamic pulse distortion.

Residual Chromatic dispersion

In general, the index of refraction of various materials, glass included, exhibits a characteristic, material related wavelength dependency resulting in a different phase velocity for each wavelength traveling through the glass fiber. The CD induced pulse distortion is due to various wavelengths comprising the bandwidth of a traveling pulse moving with different velocity. The so defined CD exhibits a mainly static behavior, which, is traditionally compensated by dispersion compensating fibers, some of which are tailored to compensate the full dispersion slope across a communication band. Residual dispersion is accumulated across a span due to slope mismatch, changes in span length, and temporal temperature variation. The wavelength dependence of the index of refraction in glass fibers is typically expressed by the Sellmeier equation[1]

$$n^2(\omega) = 1 + \sum_{j=1}^{M} \frac{B_j \omega_j^2}{\omega_j^2 - \omega^2} \qquad [1]$$

with n standing for index of refraction, ω for frequency and B_j, ω_j are empirical parameters obtained by fitting measured dispersion curves with equation [1] for M=3. Equation [1] reveals a dependency of the dynamic residual chromatic dispersion effect as defined above on the signal bandwidth.

The pulse width decreases with increasing bit-rate from about 200 ps at 2.5 Gbps to about 7 ps at 40 Gbps, corresponding to approximately 1 GHz and 26 GHz

[1] Agrawal, G.P., Fiber-Optic Communication Systems, 2nd ed. 1997, p 41

bandwidth, respectively. The increased signal bandwidth augments the dynamic effects in high-bit-rate systems making full dynamic compensation of the residual chromatic dispersion mandatory for 40 Gbps links. This temporal behavior is essentially characterized by a slow dynamic with typical minimal time constants in the range of hours and pulse distortion amounting to about 0.5 ps/km*nm at the c-band edge in a G.652 single mode fiber compensated using a WBDK-C compensating module from Lucent Technologies and about 0.1 ps/km*nm in a NZD fiber such as the TRUEWAVE-RS fiber compensated by an EHSDK-C module both from Lucent Technologies.

Polarization mode dispersion

The main phenomenon related to dynamic distortion of optical pulses in an optical communication link is the so-called polarization mode dispersion [PMD] generally resulting from the fact that a single mode fiber actually supports two propagation modes, which, may be degenerate or distinct.

An electromagnetic wave E can be described by two orthogonal components E_x and E_y defining two polarizations of the electromagnetic field.

$$E_m(z,t) = mE_o a_k \exp i(\omega t - k_m z + \Phi_m) \qquad [2]$$

where $m=x, y$, and k_m is the propagation constant.

The two waves may travel with identical propagation constant $k_x=k_y=k$ or, as the case may be in anisotropic materials exhibiting birefringence, each component propagates with a different propagation constant k_m. In the later case, a relative phase difference $\Delta\Phi = \Phi y - \Phi_x$ between the two components accumulates along the travel path resulting in both a change of the state of polarization [SOP] along the path and in case of a traveling pulse a spread of the pulse energy in time causing pulse distortion as schematically depicted in Figure 1a and 1b respectively.

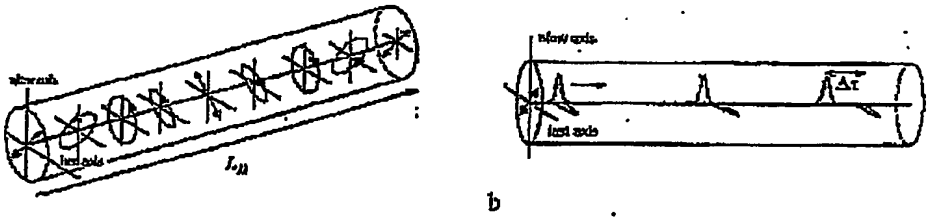

a b

Figure 1: Change of SOP and pulse spreading in a birefringent fiber section.

The SOP is typically represented in terms of Jones vectors, i.e.

$$SOP = \frac{1}{|E_0|}\begin{pmatrix} E_{0x} \\ E_{0y} \end{pmatrix} = \begin{pmatrix} a_x \exp i\Phi_x \\ a_y \exp i\Phi_y \end{pmatrix} \qquad [3]$$

with $|E_0| = \sqrt{E_{0x}^2 + E_{0y}^2}$

A glass fiber exhibits an intrinsic longitudinal anisotropy with respect to the index of refraction due to local core ellipticity induced by the manufacturing process. Figure 2 from Dyott[2] shows normalized birefringence $\Delta\overline{\beta} = \overline{\beta_f} - \overline{\beta_s}$ against normalized frequency V_b for ellipticity b/a varying from circle to slab.

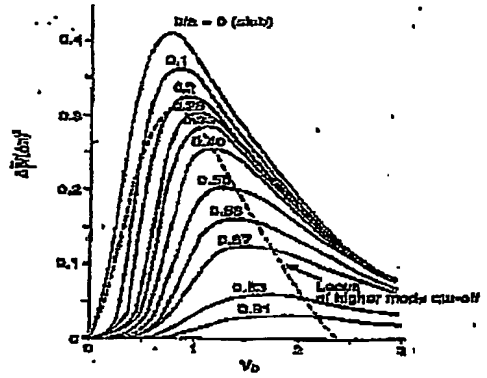

Figure 2: Normalized birefringence of elliptical waveguide (fiber optic)

The normalized birefringence $\Delta\overline{\beta}$ is the difference in the two orthogonal modal effective indices n_f and n_s. It is a function of the normalized frequency V_b and also of the core-cladding index difference Δn. All parameters constant local variations of ellipticity b/a along the propagation path z translate into longitudinal variation of the birefringence, namely the local values of n_f, n_s. The ellipticity may vary randomly both in size b/a and orientation θ along z as shown schematically in Figure 3, inducing local modulation of the refractive index.

[2] Dyott, R.B., Elliptical Fiber Waveguides, 1995, p 54

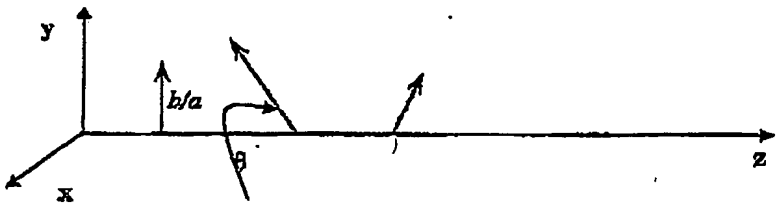

Figure 3: Variation of local ellipticity along fiber length

External and environmental effects such as local stress due to micro- or macro-bending or other forms of stress inflicted by the cabling process or field deployment contribute to the index z-anisotropy in a similar random fashion. The index anisotropy results in local birefringence variation and local coupling between the two orthogonal polarization modes *f* and *s* resulting in a spread of the time delays as depicted schematically in Figure 4 below for two birefringent sections and one mode coupling (see Figure 1b as reference for each birefringence section).

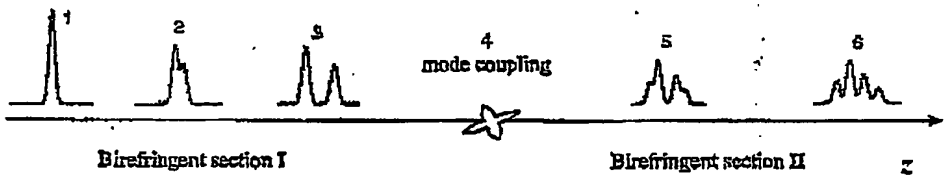

Figure 4: Time delay spread with mode coupling

Cyclic diurnal temperature variation, mechanical vibrations or other transitory environmental or external effects translate into transient local index anisotropy superimposed onto the static anisotropy described above. Consequently, the index of refraction, *n*, of a single mode fiber reflecting a multiplicity of birefringent sections and couplings may be represented by

$$n = F(\omega, x, y, z, t) \qquad [2]$$

with the frequency dependence given by equation [1].

The random character of the PMD effect was assessed experimentally in lab setups using bare or cabled fibers as well as for fibers within terrestrial and aerial deployed communication cables.

The differential group delay (DGD), defined as the relative time delay $\Delta\tau$ (see Figure 1 above) between the two orthogonal polarization components during propagation of the pulse, is typically used as the defining parameter for the estimation of PMD as follows[3].

$$\Delta\tau = \left| \frac{l}{v_{gf}} - \frac{l}{v_{gs}} \right| = l\Delta\beta \qquad [4]$$

The PMD is related to the DGD by

$$\sigma_t^2 = \left\langle (\Delta\tau)^2 \right\rangle = \frac{1}{2}\Delta\beta^2 h^2 \left[\frac{2l}{h} - 1 + \exp\left(-\frac{2l}{h} \right) \right] \qquad [5]$$

where h is the decorrelation length, namely the length at which the signal "forgets" its initial state of polarization (SOP).

When $h \ll l$ as in the case of a fiber exhibiting birefringence and mode coupling equation [4] becomes

$$\langle \Delta\tau \rangle \approx \Delta\beta\sqrt{hl} \equiv PMD\sqrt{l} \qquad [5]$$

The measured DGD values of typical fibers were found to obey a Maxwell distribution, characteristic of random 3D walk processes, which is defined by the PMD value as shown above. In a recent work[4] it was mathematically shown that typical fiber models used for numerical simulations of real optical fibers exhibiting PMD approach a Maxwellian distribution in just a few kilometers, thus confirming previous empirical/experimental results[5].

The DGD was shown to be ergodic with respect to wavelengths, fiber spans and time, namely, the DGD distribution may be determined either across wavelengths, time or fiber spans and the resultant distribution represents the whole DGD population.

Generally, the DGD is wavelength dependent, however, due to the complexity of the phenomenon a first order approximation assuming wavelength independency over the bandwidth of a single communication channel is widely employed. This first order approximation breaks down for a bandwidth, $\Delta\omega$, which is inversely proportional to the mean DGD, $\langle \Delta\tau \rangle$ and higher order PMD becomes significant.

---

[3] Agrawal, G.P., Fiber-Optic Communication Systems, 2nd ed. 1997, p 46

[4] Yang et. al., Optics Letters 26(19), 2001

[5] Gisin et. al., Pure Appl. Opt. 4, 511 (1995)

The dynamics of the PMD, assessed by a number of field tests in which the DGD of fibers of various lengths deployed in various locations was measured over extended periods of time, was reported to range between milliseconds to hours.

The transfer properties, of a fiber of length l at any given time instant t, expressed by a transfer function $G(\omega)_t$, are determined by the momentary index distribution function F_t. During a long enough time period the function F_t will go through a multiplicity of randomly distributed states F_n each generating a corresponding transfer function $G(\omega)_n$. Light pulses traveling through the fiber l during that time period will be randomly distorted reflecting the random changes of the transport properties of the medium.

An inverse Fourier transformation of the momentary transfer function $G(\omega)_n$ is the momentary impulse response $g(t)_l$ of the transfer media, i.e., the optical fiber defined by its F_n state. A pulse P_{in} injected at $z=0$ will undergo a distortion resulting in an output pulse P_{out} at l the distortion being defined by the convolution of P_{in} and $g(t)_l$

$$P_{out} = P_{in} \otimes g(t)_l \qquad [3]$$

For a pure first order approximation the impulse response is straightforward, but as already mentioned this assumption is valid only for pulse bandwidths smaller than $1/\langle \Delta\tau \rangle$ and it breaks down for single channels of 40 Gbps not to mention the bandwidth of a full [c-] band which spans about 5 THz.

Dynamic compensation schemes

Presently, dynamic compensation is approached on a channelized basis; namely, separate dynamic compensation modules are employed for individual compensation of each channel. Moreover, each type of dispersion is dealt with separately, each compensated by employing a compensation scheme based upon the same physical effect causing the dispersion.

Proposed tunable compensators for the compensation of residual chromatic dispersion due to both residual slope and time drift comprise filters based on mechanically or thermally tunable devices such as fiber Bragg gratings [FBG] with imprinted

predetermined dispersion functions, reflecting the characteristic of the effect to be compensated, tunable to within a predetermined range. Some of the proposed devices comprise channelized solutions having a bandwidth of up to 4 simultaneously tunable channels per device. Dynamic compensation modules comprise in addition to a tunable filter, also real time monitoring means for the generation of an appropriate metrics employed to efficiently converge the tunable filter. Generally, the metrics discussed are targeted at direct or indirect monitoring of chromatic dispersion effects such as RF test- tone.

The compensation of PMD is almost unanimously approached as a polarization issue[6]. The various compensation schemes[7] and theories[8] are based on per channel compensation. Namely, after demuxing each channel is individually monitored and compensated using the monitored parameter to drive a tunable compensator, some of the techniques actually involve a constant delay compensation unit. Generally, the feed-back metrics comprise polarization related effects such as the degree of polarization and the output SOP of the channel mid frequency as well as pulse related metrics such as the eye diagram quality or monitoring of a dedicated test signal sent along the link.

Figure 5 below schematically depicts the main single channel compensation schemes.

[6] Sunnerud, H. et. al. J. Lightwave Technology, March 2001
[7] Noé et.al., J. Lightwave Technology, 17(9) pp 1602, 1999
[8] Sunnerud, H. et. al. J. Lightwave Technology, 12(1) pp 50, 2000

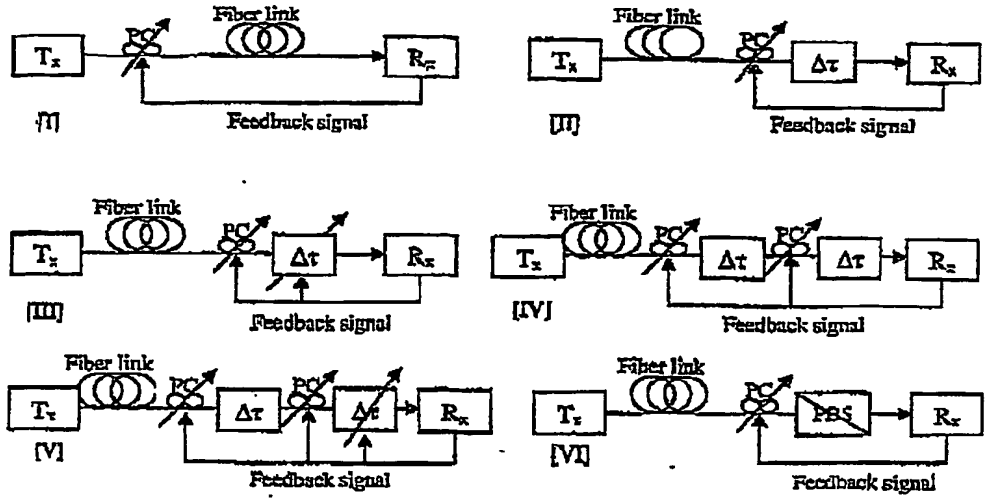

Figure 5: Single Channel PMD compensation schemes.

Where 5[I] depicts a PSP (principle state of polarization) method according to which the signal is injected in one of the system's PSP; 5[II] PC (polarization controller) and fixed delay; 5[III] PC and variable delay; 5[IV] 2PC and 2 fixed delay; 5[V] 2 PC one fixed and one variable delay and 5[VI] PC and PBS (polarization beam splitter).

These schemes are variations of the "first order PMD compensation" approach, which practically disregards higher order effects. These, however, were shown to have a major impact on the PMD compensation capability. Some of the proposed schemes may compensate for first and second order PMD[9].

Bohn[10] discusses an adaptive optical equalization approach to joined compensation of single channel dispersions using a single optical device along with electrical eye opening analysis to control the filter coefficients as opposed to approaches using different inverse filters for the compensation of the various dispersions.

[9] Mecozzi et.al.
[10] Bohn et.al., ECOC '01, 210-1

Wideband compensation approach

The wideband compensation scheme comprises a wideband filter, wideband monitoring scheme, and wideband algorithm as depicted in Figure 6 below.

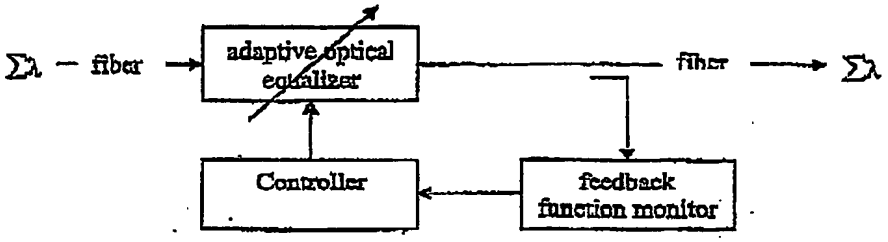

Figure 6: Schematic block diagram of a wideband dynamic compensation system

Adaptive optical equalizer

It has been shown[11] that under proper conditions a fiber may be simulated, with an assessable and caped degree of accuracy, by a discrete model. Similarly, a discrete equalizer of proper design may equalize, with an assessable and caped accuracy, a distorted signal whose distortion has been induced by its transmission through an optical link.

The adaptive optical equalizer [AOE] consists of a concatenation of a predetermined number of tunable optical filter basic units [TOFU], which comprises a tunable coupler and a tunable differential delay tap each of which may be implemented using a variety of technologies, as depicted schematically in Figure 7.

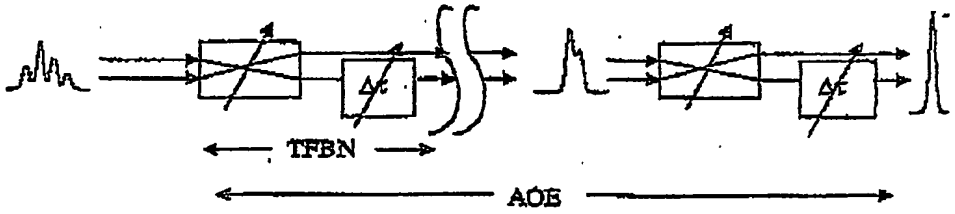

Figure 7: Schematic block diagram of an adaptive equalizer comprising a multiplicity of tunable optical filter

[11] Li, Y. et.al., J. Lightwave Technology, 18(9) pp 1205, 2000

The tunable coupler is operative in effecting a tunable, directional and selective coupling of the optical field into any number of desirable optical paths comprising the variable delay taps. Such selectivity may be based on wavelength, polarization state or any combination thereof.

The variable differential delay tap comprises one or more optical paths affecting variable time delays on each field component simultaneously. The overall effect of a TOFU is that of a controlled time-energy redistribution.

A preferable technology consists of an all-fiber filter comprised of continuously tunable delay taps connected through tunable couplers. The delay taps and couplers consist of sections of optical fiber of predetermined transfer properties and dimensions. Both the dimensions and the transfer properties may be dynamically tuned within a predefined range to generate the momentary transfer function of the adaptive optical equalizer. Preferably the adaptive optical filter exhibits an operational bandwidth equal to or greater than 30nm (approximately 5 THz) corresponding to a communication band such as the c-band extending between 1535 to 1565 nm.

Technologies such as tunable fiber Bragg gratings [FBG], tunable waveguide-arrays and liquid crystal systems may as well be employed to implement the TOFU.

Any given adaptive optical equalizer operating in conjunction with a controller to dynamically equalize a distorted pulse comprises a suitable number of TOFUs in accordance with a preferable equalizer architecture.

Monitor and monitoring scheme

A preferable feedback function monitor comprises a continuous optical domain sampling of the pulse population traveling down the link, such that at any given time the transfer function of the link across the monitored band can be estimated. The estimation rate is such as to assure a quasi-static mode with respect to the PMD dynamics. The estimated transfer function is employed to derive control parameters for driving the adaptive optical equalizer.

The pulse shape is estimated from repetitive sampling at a relatively low rate with sub-picosecond resolution. The sampling module's throughput permits characterization of multiple channels within a quasi-static regime with respect to the PMD dynamics.

The fiber's transfer function is continuously estimated from the analysis of the pulse shape of individual pulses across the monitored band.

Another preferable feedback function monitor comprises an autocorrelator, as known in the art, operative in continuously monitoring the autocorrelation function of the input and output field across the equalizer.

Control algorithm

The proposed control algorithm is a wideband, adaptive algorithm using an appropriate cost function to tune the adaptive filter in order to perform phase equalization.

Distributed link equalizer

Another aspect of the present invention is the use of the transmission link in conjunction with a centralized monitoring and control unit as a distributed adaptive equalizer operative to dynamically compensate the distortion of the transmitted pulses.

The transmission link is comprised of delay type components and couplers concatenated such that a link is operative in distorting a transmitted pulse in an uncontrolled manner. Deploying controllable elements along the link at appropriate locations thus imposing a controllable operation on the link converts it into an adaptive equalizer.

The monitoring and control unit is a central unit deployed in front of the last demux of the link and operating similarly to the monitoring and control unit described above with respect to the central equalizer and employing a similar algorithm.

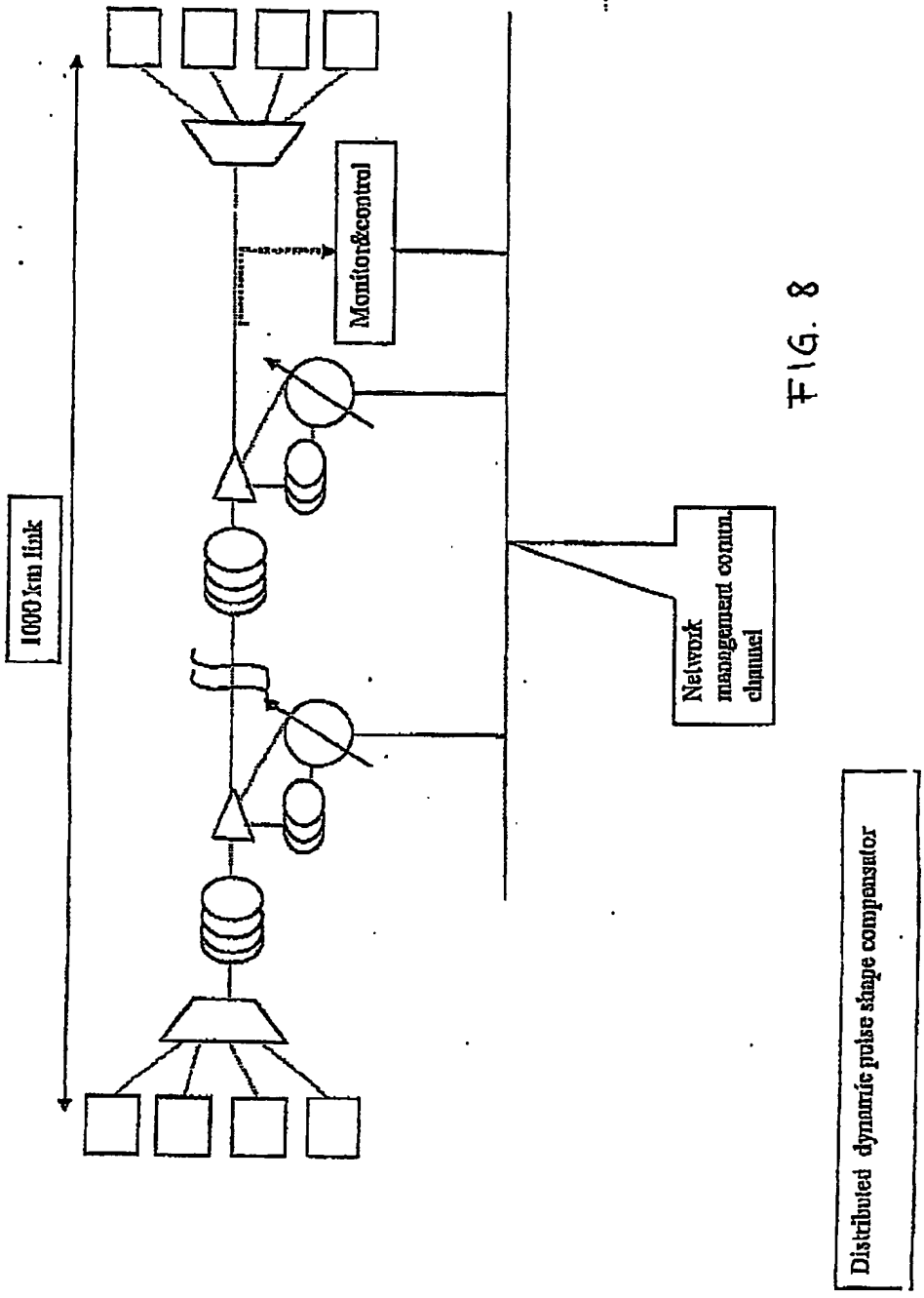
1000 km link
Monitor&control
Network management comm. channel
Distributed dynamic pulse shape compensator

FIG. 8

Assume a lattice filter comprised of two stages as depicted in fig. 9 below:

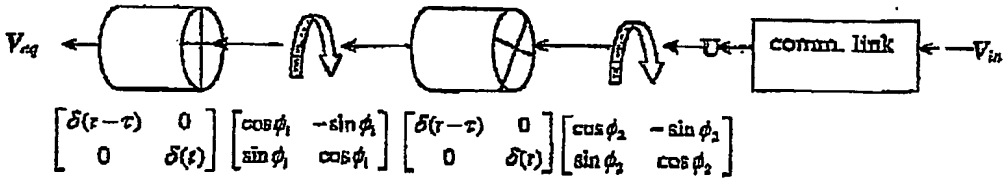

Fig. 9: 2 stage lattice filter type equalizer – schematic and matrix description

The equalizer input vector, $\mathbf{U} = [U^x \; U^y]^T$, which is the fiber output vector $\mathbf{v}_{fiberout}$ having two orthogonal polarizations x and y may be defined by [1] below in terms of subsequent delays (t), (t-τ) and (t-2τ):

$$\mathbf{U} = \left[v^x_{fiberout}(t) \;\; v^y_{fiberout}(t) \;\; v^x_{fiberout}(t-\tau) \;\; v^y_{fiberout}(t-\tau) \;\; v^x_{fiberout}(t-2\tau) \;\; v^y_{fiberout}(t-2\tau) \right]^T \quad [1]$$

The equalizer should transform the by the communication link distorted field vector $\mathbf{U}$ such that the equalizer output field $\mathbf{V}_{eq} = [V^x_{eq} \;\; V^y_{eq}]^T$ is generally equivalent to input field $\mathbf{V}_{in}$.

The equalizer output vector $\mathbf{V}_{eq}$ of the two stage equalizer of Fig. 1 may be described by equation [2]

$$\mathbf{V}_{eq} = [V^x_{eq} \;\; V^y_{eq}]^T = C\mathbf{U} \quad [2]$$

with $\mathbf{U}$ as defined in [1] and $\mathbf{C}$ defined by equation [3]

$$C = \begin{bmatrix} 0 & 0 & -s\phi_2 s\phi_1 & -c\phi_2 s\phi_1 & c\phi_2 c\phi_1 & -s\phi_2 c\phi_1 \\ s\phi_2 c\phi_1 & c\phi_2 c\phi_1 & c\phi_2 s\phi_1 & -s\phi_2 s\phi_1 & 0 & 0 \end{bmatrix} \quad [3]$$

where $s\varphi_i$, $c\varphi_i = \sin\varphi_i$, $\cos\varphi_i$ respectively.

See Appendix 1 for the derivation of matrix $\mathbf{C}$.

An appropriate metrics for any of the present channels within the link will be a function between the channel detector output, v_{equal} and the associate decision output, I_k:

$$e = \left\| v_{equal} \right\| - I_k \quad [4]$$

We want to optimize the decision making and by simple mathematical manipulation it can be shown that the updating algorithm is given by

$$\phi_i(k+1) = \phi_i(k) - \Delta \cdot e \cdot \mathbf{u}^T \left[\dot{\mathbf{C}}^T \mathbf{C} + \mathbf{C}^T \dot{\mathbf{C}} \right] \mathbf{u} \qquad [5]$$

where Δ is a small predefined constant that controls the convergence rate and $\dot{C} = \frac{\partial C}{\partial \phi_i}$.

The updating algorithm [5] is iteratively performed over few channels to find the global solution.

Extension to higher order filters is straightforward.

Other metrics, such as correlation between the input and the output of the equalizer, may be employed resulting in slightly different updating algorithms:

$$\phi_i(k+1) = \phi_i(k) - \Delta \cdot \mathbf{Q}(k) \cdot e \cdot \mathbf{u} \qquad [6]$$

where $\mathbf{Q} = \mathbf{Q}(\mathbf{C}, \dot{\mathbf{C}})$ is a scaling transformation between the measured metrics and the updating coefficient.

Numerical Examples

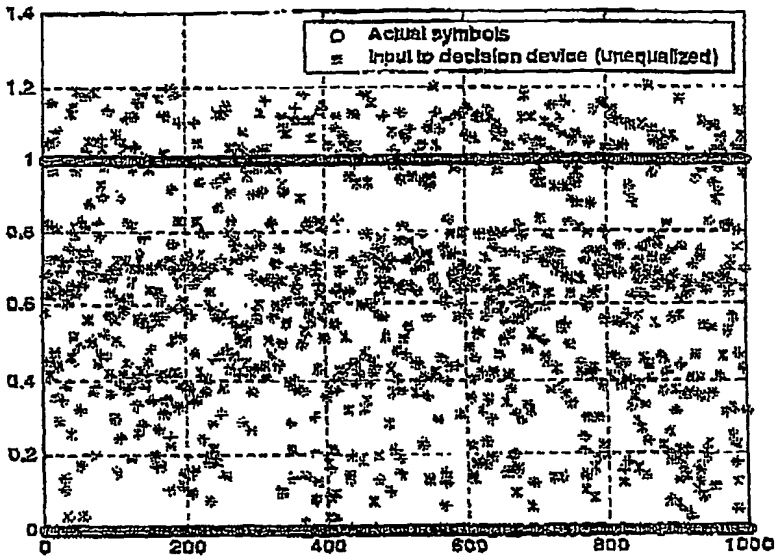

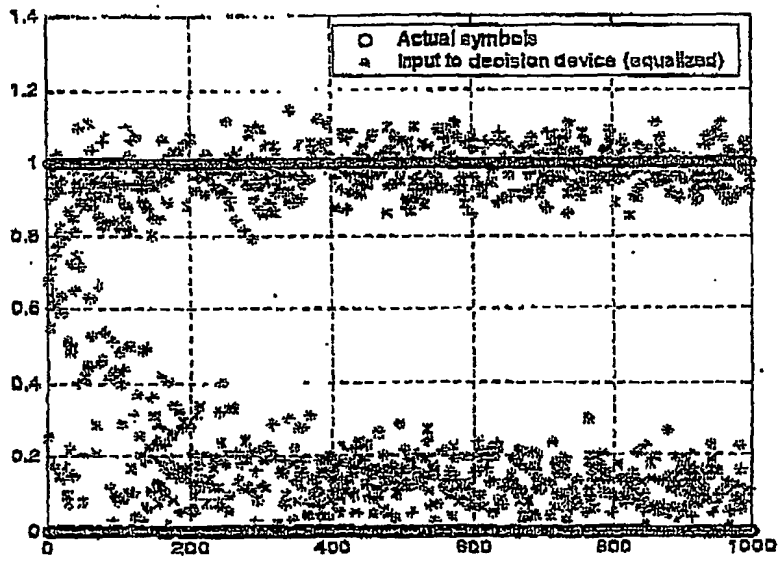

FIG. 10

Derivation example for a 2-stage equalizer:

$$V_{eq} \leftarrow \begin{bmatrix} \delta(t-\tau) & 0 \\ 0 & \delta(t) \end{bmatrix} \begin{bmatrix} \cos\phi_1 & -\sin\phi_1 \\ \sin\phi_1 & \cos\phi_1 \end{bmatrix} \begin{bmatrix} \delta(t-\tau) & 0 \\ 0 & \delta(t) \end{bmatrix} \begin{bmatrix} \cos\phi_2 & -\sin\phi_2 \\ \sin\phi_2 & \cos\phi_2 \end{bmatrix} \leftarrow$$

V^3 V^2 V^1

$$V^1 = \begin{bmatrix} c\phi_2 V^x(t) - s\phi_2 V^y(t) \\ s\phi_2 V^x(t) - c\phi_2 Vy(t) \end{bmatrix} \quad [1]$$

$$V^2 = \begin{bmatrix} c\phi_2 V^x(t-\tau) - s\phi_2 V^y(t-\tau) \\ s\phi_2 V^x(t) - c\phi_2 Vy(t) \end{bmatrix} \quad [2]$$

$$V^3 = \begin{bmatrix} c\phi_1 c\phi_2 V^x(t-\tau) - c\phi_1 s\phi_2 V^y(t-\tau) - s\phi_1 s\phi_2 V^x(t) - s\phi_1 c\phi_2 V^y(t) \\ s\phi_1 c\phi_2 V^x(t-\tau) - s\phi_1 s\phi_2 V^y(t-\tau) + c\phi_1 s\phi_2 V^x(t) + c\phi_1 c\phi_2 V^y(t) \end{bmatrix} \quad [3]$$

$$V_{eq} = \begin{bmatrix} c\phi_1 c\phi_2 V^x(t-2\tau) - c\phi_1 s\phi_2 V^y(t-2\tau) - s\phi_1 s\phi_2 V^x(t-\tau) - s\phi_1 c\phi_2 V^y(t-\tau) \\ s\phi_1 c\phi_2 V^x(t-\tau) - s\phi_1 s\phi_2 V^y(t-\tau) + c\phi_1 s\phi_2 V^x(t) + c\phi_1 c\phi_2 V^y(t) \end{bmatrix} \quad [4]$$

$$= \begin{bmatrix} 0 & 0 & -s\phi_1 s\phi_2 & -s\phi_1 s\phi_2 & c\phi_1 c\phi_2 & -c\phi_1 s\phi_2 \\ c\phi_1 s\phi_2 & c\phi_1 c\phi_2 & s\phi_1 c\phi_2 & -s\phi_1 s\phi_2 & 0 & 0 \end{bmatrix} \begin{bmatrix} V^x(t) \\ Vy(t) \\ V^x(t-\tau) \\ Vy(t-\tau) \\ V^x(t-2\tau) \\ V^y(t-2\tau) \end{bmatrix} =$$

$$= CU$$

Main claim:

A method for instantaneous generation of optical filter configurations for the dynamic equalization of distorted optical communication signals transmitted in an optical communication link in response to a time-varying error-signal said method comprising:

1. incorporating adaptive optical filter units at appropriate locations within the link
2. generating an error-signal representative of the instantaneous signal distortion
3. changing the adaptive parameters of the filter units in response to the error-signal generating an instantaneous filter configuration